Draft version February 5, 2008
Preprint typeset using LaTeX style emulateapj v. 5/14/03

arXiv:astro-ph/0512233v5 14 Feb 2006

THE DEEP2 GALAXY REDSHIFT SURVEY: CLUSTERING OF GALAXIES AS A FUNCTION OF LUMINOSITY AT $Z = 1$

Alison L. Coil[1,2], Jeffrey A. Newman[1,3], Michael C. Cooper[4], Marc Davis[4], S. M. Faber[5], David C. Koo[5], Christopher N. A. Willmer[2,5]

Draft version February 5, 2008

ABSTRACT

We measure the clustering of DEEP2 galaxies at $z = 1$ as a function of luminosity on scales 0.1 h^{-1} Mpc to 20 h^{-1} Mpc. Drawing from a parent catalog of 25,000 galaxies at $0.7 < z < 1.3$ in the full DEEP2 survey, we create volume-limited samples having upper luminosity limits between $M_B = -19$ and $M_B = -20.5$, roughly $0.2 - 1L^*$ at $z = 1$. We find that brighter galaxies are more strongly clustered than fainter galaxies and that the slope of the correlation function does not depend on luminosity for $L < L^*$. The brightest galaxies, with $L > L^*$, have a steeper slope. The clustering scale-length, r_0, varies from 3.69 ± 0.14 for the faintest sample to 4.43 ± 0.14 for the brightest sample. The relative bias of galaxies as a function of L/L^* is steeper than the relation found locally for SDSS galaxies (Zehavi et al. 2005) over the luminosity range that we sample. The absolute bias of galaxies at $z \sim 1$ is scale-dependent on scales $r_p < 1$ h^{-1} Mpc, and rises most significantly on small scales for the brightest samples. For a concordance cosmology, the large-scale bias varies from 1.26 ± 0.04 to 1.54 ± 0.05 as a function of luminosity and implies that DEEP2 galaxies reside in dark matter halos with a minimum mass of $\sim 1 - 3 \times 10^{12} h^{-1}\mathrm{M}_\odot$.

Subject headings: galaxies: high-redshift — cosmology: large-scale structure of the universe

1. INTRODUCTION

The clustering of galaxies has long been used as a fundamental measure of the large-scale structure of the universe. Clustering measures place strong constraints on galaxy formation and evolution models and provide estimates of the average or minimum parent dark matter halo mass of a given galaxy population, allowing placement in a cosmological context (e.g., Mo & White 1996; Sheth & Tormen 1999). Locally, large surveys such as the 2-Degree Field Galaxy Redshift Survey (2dFGRS) and the Sloan Digital Sky Survey (SDSS) have measured the two-point correlation function of galaxies precisely enough to allow detailed halo occupation distribution (HOD) modeling (e.g., Phleps et al. 2005; Yan, Madgwick, & White 2003; Yang et al. 2005; Zehavi et al. 2005), as well as cosmological parameter constraints (e.g., Abazajian et al. 2005; Peacock et al. 2001).

In this paper we focus on the observed clustering of galaxies as a function of luminosity. Both 2dF and SDSS have found that at $z \sim 0.1$ brighter galaxies cluster more strongly, with the relative bias on large scales increasing linearly with luminosity (e.g., Alimi, Valls-Gabaud, & Blanchard 1988; Benoist et al. 1996; Hamilton 1988; Norberg et al. 2001, 2002; Willmer, da Costa, & Pellegrini 1998; Zehavi et al. 2004). A simple interpretation is that brighter galaxies reside in more massive dark matter halos, which are more clustered in the standard theories of hierarchical structure formation. The full galaxy samples for these surveys are generally unbiased with respect to the dark matter density field on large scales (e.g., Croton et al. 2004; Peacock et al. 2001; Verde et al. 2002).

Locally, the two-point correlation function is relatively well-fit by a power law, $\xi(r)=(r/r_0)^{-\gamma}$, with $r_0 \sim 5$ h^{-1} Mpc and $\gamma \sim 1.8$ (e.g., Norberg et al. 2002; Zehavi et al. 2005). Small deviations from a power law have recently been detected on scales $r < 10$ h^{-1} Mpc and can be naturally be explained in the HOD framework as the transition between pairs of galaxies within the same halo (the 'one-halo' term) on small scales and galaxies in different halos (the 'two-halo' term) on larger scales (Zehavi et al. 2004). The largest deviations are seen for the brightest galaxy samples, with $L > L^*$. These galaxies are generally found in groups and clusters, which have larger 'one-halo' terms due to the many galaxies residing in a single parent dark matter halo and therefore have a steeper correlation slope on small scales.

Lyman-break galaxies (LBGs) at $z \sim 3 - 4$ also display a luminosity-dependence in their clustering properties (Allen et al. 2005; Lee et al. 2005; Ouchi et al. 2005). The large-scale bias of LBGs ranges from $\sim 3 - 8$, depending on the luminosity of the sample. There is also a strong scale-dependence to the bias on small scales, where the correlation function rises sharply below $r \sim 0.5$ h^{-1} Mpc(Lee et al. 2005; Ouchi et al. 2005). This rise has been interpreted as evidence for multiple LBGs residing in single dark matter halos at $z \sim 4$.

In this paper, we present results on the luminosity-dependent clustering of galaxies at $z \sim 1$, using the nearly-completed DEEP2 Galaxy Redshift Survey. The data sample used here is 10 times larger than our initial results presented in Coil et al. (2004a) and represents the most robust measurements of $\xi(r)$ at $z > 0.7$ to date. In future papers we will address clustering properties

---

[1] Hubble Fellow

[2] Steward Observatory, University of Arizona, Tucson, AZ 85721

[3] Institute for Nuclear and Particle Astrophysics, Lawrence Berkeley National Laboratory, Berkeley, CA 94720

[4] Department of Astronomy, University of California, Berkeley, CA 94720

[5] University of California Observatories/Lick Observatory, Department of Astronomy and Astrophysics, University of California, Santa Cruz, CA 95064

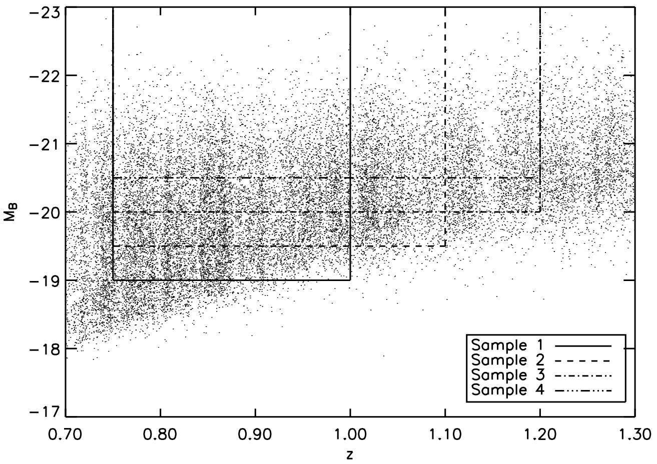

FIG. 1.— Absolute B-band magnitude (in AB magnitudes, with $h = 1$) versus redshift for the parent DEEP2 galaxy catalog. The magnitude and redshift ranges of the four samples used here are shown, and properties of each sample are given in Table 1.

as a function of other galaxy properties such as color, stellar mass and redshift; here we focus solely on the luminosity-dependence. We choose to use integral, rather than differential, luminosity bins to facilitate comparison with theoretical models (e.g., Kravtsov et al. 2004; Tinker et al. 2005). Luminosity-threshold samples are preferred for HOD modeling, as theoretical predictions for HODs have been studied more extensively for mass (luminosity) thresholds and afford fewer parameters to fit than differential bins (for details see e.g. Zehavi et al. 2005). In this case the HOD has a relatively simple form, e.g., the mean occupation function is a step function (for central galaxies) plus a power law (for satellites). The outline of the paper is as follows: §2 briefly describes the DEEP2 survey and data sample. In §3 we outline the methods used in this paper, while §4 presents our results on the luminosity-dependence of galaxy clustering at $z \sim 1$. In §5 we discuss the galaxy bias and the relative biases between our luminosity samples and conclude in §6.

2. DATA SAMPLE

The parent galaxy sample used here is from the DEEP2 Galaxy Redshift Survey, a three-year project using the DEIMOS spectrograph (Faber et al. 2003) on the 10-m Keck II telescope to survey optical galaxies at $z \simeq 1$ in a comoving volume of approximately $5\times10^6\ h^{-3}$ Mpc^3. Using $\sim$ 1 hour exposure times, the survey has measured redshifts for $\sim 30,000$ galaxies in the redshift range $0.7 \sim z \sim 1.45$ to a limiting magnitude of $R_{\rm AB} = 24.1$ (Davis et al. 2003; Faber et al. 2006). The survey covers three square degrees of the sky over four widely separated fields to limit the impact of cosmic variance. Fields consist of two to four adjacent pointings of size 0.5×0.67 degrees each. Details of the DEEP2 observations, catalog construction and data reduction can be found in Davis et al. (2003), Coil et al. (2004b), Davis, Gerke, & Newman (2004), and Faber et al. (2006). Here we use the full sample from ten pointings in all four fields to create four nearly volume-limited samples as a function of Johnson B absolute magnitude (M_B).

TABLE 1. DETAILS OF DEEP2 GALAXY LUMINOSITY SAMPLES

	No. of galaxies	n ($h^3 Mpc^{-3}$)	M_B range	Median M_B	z range	Mean z
1	10530	$1.3\ 10^{-2}$	≤ -19.0	-20.28	$0.75 - 1.0$	0.87
2	11023	$8.4\ 10^{-3}$	≤ -19.5	-20.41	$0.75 - 1.1$	0.92
3	9526	$4.9\ 10^{-3}$	≤ -20.0	-20.64	$0.75 - 1.2$	0.98
4	5418	$2.5\ 10^{-3}$	≤ -20.5	-20.96	$0.75 - 1.2$	0.99

Fig. 1 shows the absolute magnitude and redshift of each galaxy in the parent catalog and the regions from which the different luminosity samples were drawn. The three brightest samples (with limiting magnitudes down to $M_B = -19.5$) are volume-limited for blue galaxies, while the faintest sample is missing some fainter blue galaxies at $z \gtrsim 0.95$. The samples are not entirely volume-limited for red galaxies, due to the $R_{\rm AB}$ selection of the DEEP2 survey (see Willmer et al. (2006) for definitions of blue and red galaxies and a discussion of this selection effect). K-corrections are calculated as described in Willmer et al. (2006); we do not include corrections for luminosity evolution. Table 1 lists the details of each luminosity sample. To convert measured redshifts to comoving distances along the line of sight we assume a flat ΛCDM cosmology with $\Omega_{\rm m} = 0.3$ and $\Omega_\Lambda = 0.7$. We define $h \equiv H_0/(100\ {\rm km\ s^{-1}\ Mpc^{-1}})$ and quote correlation lengths, r_0, in comoving h^{-1} Mpc. All absolute magnitudes are AB with $h = 1$.

3. METHODS

Details of the methods used to measure the correlation function are given in Coil et al. (2004a, 2006); we repeat the most relevant details here. The two-point correlation function $\xi(r)$ is defined as a measure of the excess probability above Poisson of finding an object in a volume element dV at a separation r from another randomly chosen object,

$$dP = n[1 + \xi(r)]dV, \tag{1}$$

where n is the mean number density of the object in question (Peebles 1980).

We measure the two-point correlation function using the Landy & Szalay (1993) estimator,

$$\xi = \frac{1}{RR}\left[DD\left(\frac{n_R}{n_D}\right)^2 - 2DR\left(\frac{n_R}{n_D}\right) + RR\right], \tag{2}$$

where DD, DR, and RR are pair counts of galaxies in the data-data, data-random, and random-random catalogs, and n_D and n_R are the mean number densities of galaxies in the data and random catalogs. The random catalog has the same overall sky coverage and redshift distribution as the data and serves as an unclustered sample with which to compare the data. The spatial window function of the DEEP2 survey is applied to the random catalog, which includes masking areas around bright stars and taking into account the varying redshift completeness of our observed slitmasks.

Distortions in ξ are introduced parallel to the line of sight due to peculiar velocities of galaxies. In order to uncover the real-space clustering properties, we measure ξ

in two dimensions, as a function of distance both perpendicular to (r_p) and along (π) the line of sight. As redshift-space distortions affect only the line-of-sight component of ξ, integrating over the π direction leads to the projected correlation function $w_p(r_p)$, which is independent of redshift-space distortions. Following Davis & Peebles (1983),

$$w_p(r_p) = 2\int_0^\infty d\pi\ \xi(r_p,\pi) = 2\int_0^\infty dy\ \xi(r_p^2+y^2)^{1/2}, \tag{3}$$

where y is the real-space separation along the line of sight. We sum $\xi(r_p,\pi)$ to a maximum separation of $\pi = 20\ h^{-1}$ Mpc and measure $w_p(r_p)$ as a function of scale for $0.1 < r_p < 20\ h^{-1}$ Mpc. Errors on $w_p(r_p)$ are calculated using the standard error across the 10 separate data pointings. We estimate the integral constraint numerically using the random catalog (see e.g., Eqn. 8 of Roche and Eales 1999) and find it to be ~0.1 and therefore negligible.

If $\xi(r)$ is modeled as a power-law, $\xi(r) = (r/r_0)^{-\gamma}$, then r_0 and γ can be readily extracted from the projected correlation function, $w_p(r_p)$, using an analytic solution to Equation 3:

$$w_p(r_p) = r_p\left(\frac{r_0}{r_p}\right)^\gamma \frac{\Gamma(\frac{1}{2})\Gamma(\frac{\gamma-1}{2})}{\Gamma(\frac{\gamma}{2})}, \tag{4}$$

where Γ is the gamma function. A power-law fit to $w_p(r_p)$ will then recover r_0 and γ for the real-space correlation function, $\xi(r)$. We correct for the covariance between r_p bins when calculating the errors on r_0 and γ.

To correct for undersampling of galaxies on small scales due to our slitmask target selection algorithm we use the mock galaxy catalogs of Yan, White, & Coil (2004). We create samples with identical redshift and luminosity ranges as each data sample and measure the ratio of the projected correlation function in the mock catalogs for catalogs with and without the slitmask target selection algorithm applied. We then multiply the measured $w_p(r_p)$ in the data by this ratio, which is a smooth function of both scale and luminosity. We note that using mock catalogs with different HOD parameters does not change our results (Coil et al. 2006). Both the observed and corrected data are shown in this paper.

4. CLUSTERING AS A FUNCTION OF LUMINOSITY

Fig. 2 shows the measured projected correlation function for each luminosity sample as a function of scale, for $r_p = 0.1 - 20\ h^{-1}$ Mpc. The left panel shows the observed $w_p(r_p)$, while the right panel shows $w_p(r_p)$ after correcting for slitmask target selection effects. The corrections are larger for the brighter samples and are most significant on scales less than $r_p = 0.3\ h^{-1}$ Mpc. Errors are calculated using the standard error across the ten individual DEEP2 pointings. Amplitudes and errors for $w_p(r_p)$ are given for each of the luminosity samples at four different scales in Table 2.

Power-law fits to the corrected $w_p(r_p)$ are performed for a range of scales: the full range shown here ($0.1 < r_p < 20\ h^{-1}$ Mpc), smaller scales ($0.1 < r_p < 1\ h^{-1}$ Mpc), and larger scales ($1 < r_p < 20\ h^{-1}$ Mpc). Values of r_0 and γ are given in Table 2 for each r_p range and results for the full range are shown in Fig. 3. Errors on r_0 and γ are estimated using jacknife errors across the ten samples; this approach includes the covariance between adjacent r_p bins and results in errors which are 2-3 times higher than the formal $1-\sigma$ statistical errors of the least-squares fit to the data, assuming the r_p bins are independent. Fitting for a power law on larger scales, $1 < r_p < 20\ h^{-1}$ Mpc, results in r_0 and γ values within the quoted 1-σ errors for the full range, as shown in Table 2, and fits to the observed data without corrections for slitmask effects result in 2% lower values of r_0 and γ for the full range for all samples except the brightest, where the difference is 3% in both r_0 and γ.

We show in Fig. 4 deviations from the best-fit power law over all scales for each luminosity sample. A power law fits the data reasonably well on scales $r_p > 1\ h^{-1}$ Mpc, but all samples depart from power-law behavior at small scales ($r_p < 0.4\ h^{-1}$ Mpc). These deviations can be explained naturally by a halo occupation approach to modeling the observed clustering; we will present HOD fits to these data in a separate paper.

The clustering scale length, r_0, is significantly larger for the brighter samples; r_0 increases from 3.69 ± 0.14 to 4.43 ± 0.14 over the luminosity ranges shown here. The slope is $\sim 1.73 \pm 0.03$ for each of the three samples with $L \leq L^*$ and increases to $\gamma = 1.82 \pm 0.03$ for the brightest $L > L^*$ sample (at $z = 1$, $M^* = -20.7$ in our magnitude units; cf. Willmer et al. 2006). This increase in γ is found on both small ($r_p < 1\ h^{-1}$ Mpc) and large ($r_p > 1\ h^{-1}$ Mpc) scales. We note that the ratio of red to blue galaxies is not widely different between the samples: 76% of the galaxies are blue in the faintest sample while 67% are blue in the brightest sample (see Fig. 4 of Willmer et al. (2006) for a color-magnitude diagram of DEEP2 galaxies).

As shown in Fig. 6 of Conroy, Wechsler, & Kravtsov (2006), the clustering results presented here are well-fit by a simple model in which luminosities are assigned to dark matter halos and sub-halos in an N-body simulation by matching the observed DEEP2 luminosity function (Willmer et al. 2006) to the sub-halo/halo circular velocity function (as a proxy for mass), with no free parameters. Every sub-halo with mass $M > 1.6 \times 10^{10} h^{-1} M_\odot$ (the resolution limit of the halo catalog) is assumed to have a galaxy at the center; therefore the radial distribution of galaxies matches that of the sub-halos. This relatively simple model correctly reproduces our clustering measurements as a function of luminosity and scale presented here, on scales $r_p = 0.1 - 10\ h^{-1}$ Mpc, and implies that brighter galaxies reside in more massive dark matter halos.

5. GALAXY BIAS

We now calculate the relative bias of each luminosity sample with respect to the $M_B < -20.0$ sample, which has a median luminosity near L^* ($M^* = -20.7$ at $z = 0.9$; see Willmer et al. (2006)). The relative bias is defined as the square root of the ratio of $w_p(r_p)$ for a given sample divided by $w_p(r_p)$ for the $M_B < -20.0$ sample. We calculate the relative bias at two scales, $r_p = 0.1\ h^{-1}$ Mpc and $r_p = 2.7\ h^{-1}$ Mpc, using the power-law fits given in Table 2 for small and large scales. Fig. 5 plots the relative bias as a function of median absolute magnitude (bottom axis) and L/L^* (top axis) at $r_p = 0.1\ h^{-1}$ Mpc (left) and $r_p = 2.7\ h^{-1}$ Mpc (right). There

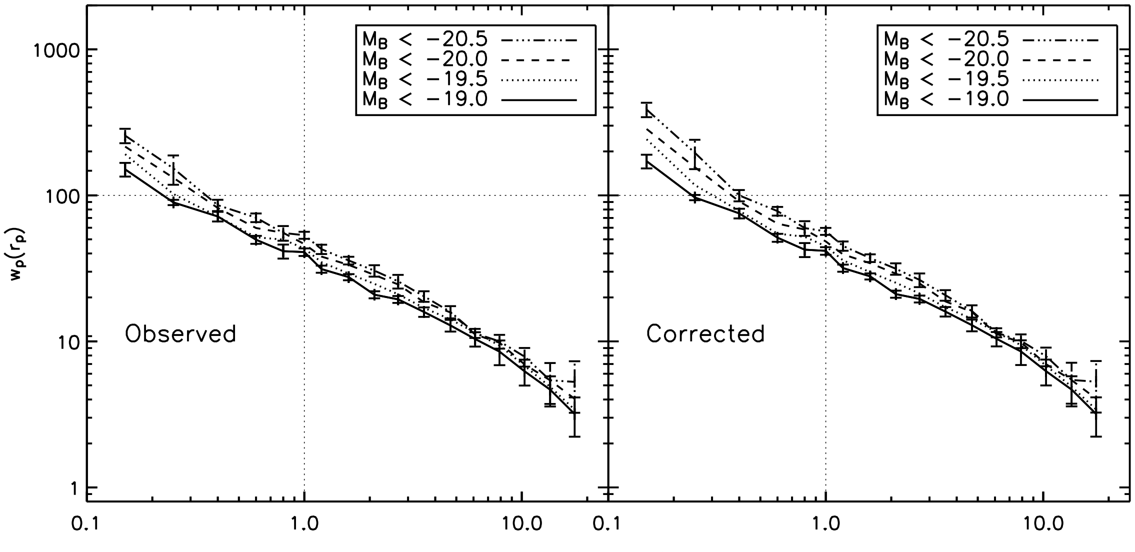

FIG. 2.— Projected two-point correlation function, $w_p(r_p)$, of DEEP2 galaxies for different luminosity samples. The observed $w_p(r_p)$ is shown in the left panel, while on the right we have corrected for the slitmask target selection effects using mock catalogs. Fiducial lines at $r_p = 1$ h^{-1} Mpc and $w_p(r_p)$= 100 have been drawn to guide the eye.

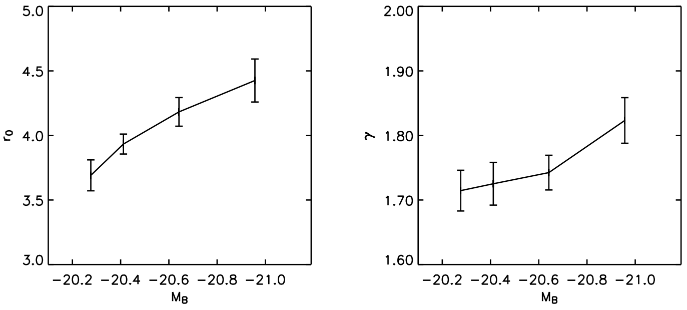

FIG. 3.— The clustering scale-length, r_0 (left), and slope, γ (right), of DEEP2 galaxies as a function of the median absolute magnitude of each sample. The values of r_0 and γ for each sample are given in Table 2.

TABLE 2. PROJECTED CORRELATION FUNCTION AMPLITUDES FOR LUMINOSITY SAMPLES

	w_p at r_p in h^{-1} Mpc			
	$r_p = 0.15$	$r_p = 1.0$	$r_p = 4.7$	$r_p = 10.3$
1	171 ± 18	41.7 ± 2.5	12.9 ± 1.2	6.2 ± 1.3
2	242 ± 29	44.8 ± 3.3	14.2 ± 1.2	6.8 ± 1.3
3	285 ± 27	48.3 ± 4.2	15.9 ± 0.9	7.0 ± 1.1
4	387 ± 44	56.7 ± 3.1	16.1 ± 1.5	7.9 ± 1.2

NOTE. — These values have all been corrected for slitmask target selection effects.

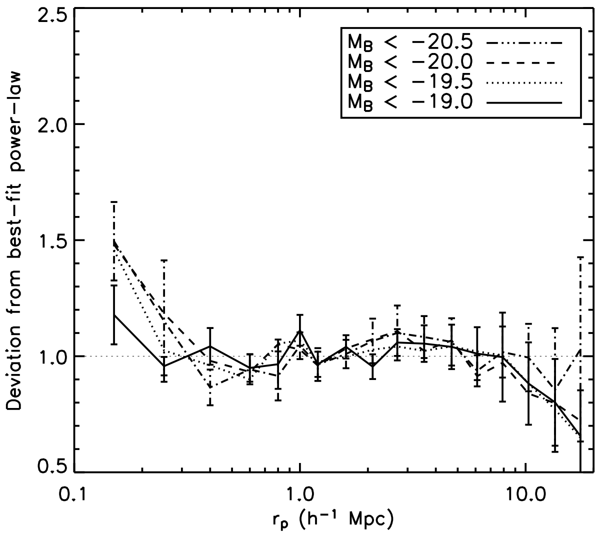

FIG. 4.— Deviations of $w_p(r_p)$ from the best-fit power law for each luminosity sample as a function of scale, using the values of r_0 and γ listed in Table 2. A thin dotted line is drawn for reference at $y = 1$.

is a linear trend of bias with luminosity on both small and large scales, though the trend is stronger on smaller scales.

In the right panel, we also show for comparison the bias of SDSS galaxies as a function of $L/L*$ measured by Zehavi et al. (2005) on the same scale, $r_p = 2.7$ h^{-1} Mpc. The bias of galaxies is a stronger function of L/L^* at $z \sim 1$ compared to $z \sim 0$ over the luminosity range that we sample here.

We further calculate the absolute bias of each sample, using the ratio of the observed galaxy clustering to the clustering expected for the underlying dark matter density field. To estimate the dark matter correlation function, we use the power spectrum provided by the publicly available code of Smith et al. (2003), for a cosmology with $\Omega_m = 0.3, \Omega_\Lambda = 0.7, \sigma_8 = 0.9$, and $\Gamma = 0.21$. Smith et al. (2003) analyze the non-linear evolution of clustering in a large library of N-body cosmological simulations, including small scales where merging of dark matter halos is important. They use an an-

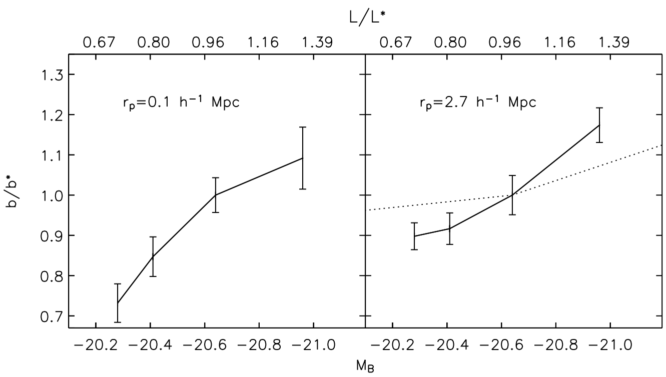

FIG. 5.— The mean relative bias of each of our samples compared to the $M_B < -20.0$ sample. The relative bias increases linearly with luminosity, though the trend is stronger on smaller scales (left) than larger scales (right). The dotted line in the right panel shows the same relation from Zehavi et al. (2005) in SDSS galaxies at $z \sim 0.1$ as a function of L/L^*, shown in the upper axis.

alytic halo-model approach to fit the non-linear structure evolution, which is more accurate than the popular Peacock & Dodds (1994) prescription; we include a 5% error on the dark matter $w_p(r_p)$ in our calculation of the absolute bias to reflect the uncertainty in the fit. We do not include an additional uncertainty in the cosmological parameters; for $\sigma_8 = 0.8$ the large-scale bias is 13% higher, while for $\sigma_8 = 1.0$ it is 10% lower. The results are shown in Fig. 6. While there is no significant scale-dependence to the bias on scales $r_p > 1$ h^{-1} Mpc, all four samples show a dip in the bias on scales $r_p \sim 0.3 - 0.8$ h^{-1} Mpc and a rise on small scales below $r_p \sim 0.1$ h^{-1} Mpc. On scales of $r_p = 1 - 10$ h^{-1} Mpc, the mean absolute bias ranges from $b = 1.26 \pm 0.04$ for the $M_B < -19$ sample to $b = 1.54 \pm 0.05$ for the $M_B < -20.5$ sample; values are listed in Table 2. On the smallest scales we measure here, $r_p = 0.1$ h^{-1} Mpc, the bias ranges from $b = 1.2 \pm 0.1$ for the $M_B < -19$ sample to $b = 1.9 \pm 0.2$ for the $M_B < -20.5$ sample.

We note that the absolute biases measured here are larger than in Coil et al. (2004a) (though within 1σ, given the error on that result), where we measured the clustering of all DEEP2 galaxies in the first completed pointing. This is simply due to cosmic variance: galaxies in that pointing exhibit lower clustering than the mean of the completed DEEP2 survey; that region happened to be less clustered than average.

From these large-scale bias measurements we can estimate the minimum dark matter halo mass that each galaxy sample resides in, on average, where the mass is defined as the mass enclosed in a region that is 200 times the critical density. Using the formulae of Sheth & Tormen (1999) for $\Omega_m = 0.3, \Omega_\Lambda = 0.7$, and $\sigma_8 = 0.9$, we find that the minimum dark matter mass for our samples ranges from $\sim 9 \times 10^{11} - 3 \times 10^{12} h^{-1}\mathrm{M}_\odot$ (values are listed in Table 2).

We compare our results with those of the Vimos-VLT Deep Survey (VVDS). Marinoni et al. (2005) measure the luminosity-dependence of the galaxy bias averaged on scales 5-10 h^{-1} Mpc using a sample 1044 VVDS galaxies in an area of 0.16 square degrees between $0.7 < z < 0.9$. They find that the bias is 1.02 ± 0.20 and 1.14 ± 0.21 for luminosity thresholds of $M_B < -18.7$ and $M_B < -20$, where the quoted errors include the statistical error only and do not include the dominant error due to cosmic variance. Their bias values are lower than those shown here but are likely within the errors if cosmic variance is included. Additionally, a more recent VVDS paper on the luminosity-dependence of galaxy clustering at $0.5 < z < 1.2$ (Pollo et al. 2006) yields correlation amplitudes and slopes that are similar to ours, but with a steeper trend in $b/b*$; they find lower r_0 values for the fainter samples ($r_0 = 2.95 \pm 0.34$ for $M_B < -19$) and higher r_0 values for the brighter samples ($r_0 = 5.01 \pm 1.5$ for $M_B < -21$) and a stronger change in correlation slope γ with luminosity than is found here. However, given the cosmic variance errors in the results, which use a sample of ~3300 galaxies with $M_B < -19$ covering an area of 0.49 square degrees, the differences are not significant.

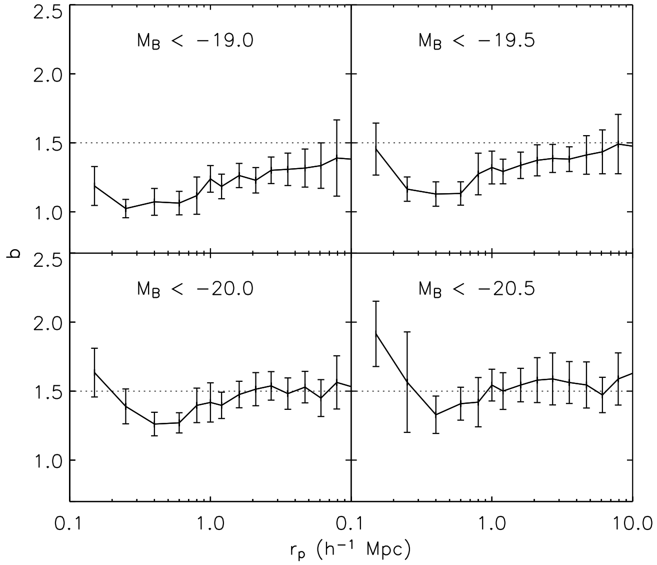

FIG. 6.— The absolute bias of DEEP2 galaxies for a σ_8=0.9 ΛCDM cosmology as a function of scale for each of our luminosity samples. The bias is derived using the ratio of the observed galaxy clustering to the Smith et al. (2003) fitting function for the clustering of dark matter halos at the same redshifts. There is a clear scale-dependence to the bias for $r_p < 1$ h^{-1} Mpc. The bias on scales $r_p > 1$ h^{-1} Mpc increases with luminosity and is relatively scale-independent.

6. CONCLUSIONS

Using volume-limited subsamples of the 25,000 galaxies with spectroscopic redshifts between $0.7 \leq z \leq 1.4$ from the nearly-completed DEEP2 Galaxy Redshift Survey, we have measured the clustering of galaxies as a function of luminosity at $z \sim 1$. We find that the clustering scale length, r_0, increases linearly with luminosity over the range sampled here and that the bias of clustering relative to L^* is strong to what is found at $z \sim 0$. The brightest DEEP2 sample, with $L > L*$, has a significantly steeper correlation slope ($\gamma = 1.82 \pm 0.03$) on all scales than the fainter luminosity samples, which all have similar slopes of $\gamma \sim 1.73$. This is not due to differences in the mix of galaxies in each sample; the red galaxy fraction depends only weakly on luminosity in the DEEP2 data.

Conroy, Wechsler, & Kravtsov (2006) attempt to model the clustering results presented here with a simple prescription in which luminosities are assigned to dark

Table 3. Clustering Results for Luminosity Samples

	r_0[a] h^{-1} Mpc	γ	r_0[b] h^{-1} Mpc	γ	r_0[c] h^{-1} Mpc	γ	b[d]	M_{min} $h^{-1}M_\odot$
1	3.69 ± 0.14	1.71 ± 0.03	3.78 ± 0.23	1.68 ± 0.04	3.76 ± 0.09	1.76 ± 0.05	1.26 ± 0.04	$9.0\ 10^{11}$
2	3.93 ± 0.10	1.73 ± 0.03	3.73 ± 0.19	1.80 ± 0.05	3.97 ± 0.10	1.74 ± 0.06	1.36 ± 0.04	$1.4\ 10^{12}$
3	4.18 ± 0.08	1.74 ± 0.03	3.67 ± 0.11	1.93 ± 0.06	4.25 ± 0.12	1.76 ± 0.07	1.48 ± 0.04	$2.2\ 10^{12}$
4	4.43 ± 0.14	1.82 ± 0.03	4.21 ± 0.22	1.90 ± 0.09	4.47 ± 0.11	1.84 ± 0.05	1.54 ± 0.05	$2.8\ 10^{12}$

[a] for scales $r_p = 0.1 - 20\ h^{-1}$ Mpc
[b] for scales $r_p = 0.1 - 1\ h^{-1}$ Mpc
[c] for scales $r_p = 1 - 20\ h^{-1}$ Mpc
[d] large-scale bias ($r_p = 1 - 10\ h^{-1}$ Mpc)

matter halos and sub-halos in an N-body simulation by matching the observed DEEP2 luminosity function to the sub-halo/halo maximum circular velocity, used as a proxy for mass. Their model fits our data extremely well, implying that brighter galaxies reside in more massive dark matter halos and that the luminosity-dependent clustering is dominated by the physical distribution of halos on large scales and sub-halos on small scales, as a function of mass. It is remarkable that the results presented in this paper can be explained using a model in which the luminosity of a galaxy depends solely on the mass of the dark matter halo in which it resides.

The mean galaxy bias in the DEEP2 data on scales $r_p = 1 - 10\ h^{-1}$ Mpc for a concordance cosmology ranges from 1.26 ± 0.04 to 1.54 ± 0.05 as a function of luminosity for $L/L^* = 0.7 - 1.3$, and there is a scale-dependence to the bias for $r_p < 1\ h^{-1}$ Mpc. The brightest samples show the strongest rise in the correlation function on small scales, which is likely due to these galaxies preferentially residing in groups. This upturn on small scales has also been seen both locally for SDSS galaxies with $L > L^*$ (Zehavi et al. 2005) and at high redshift for LBG galaxies at $z \sim 3 - 4$ (Lee et al. 2005; Ouchi et al. 2005). The strength of the rise in the DEEP2 sample is smaller than what is found at $z \sim 3 - 4$, as expected from simulations (Kravtsov et al. 2004), and the large-scale bias is intermediate between the bias of LBGs and local galaxies of similar L/L^* in 2dF and SDSS.

We thank Scott Burles, Charlie Conroy, Darren Croton, Daniel Eisenstein and Zheng Zheng for helpful discussions. We also thank the referee for useful comments. This project was supported by the NSF grant AST-0071048. A.L.C. and J.A.N. are supported by NASA through Hubble Fellowship grants HF-01182.01-A and HST-HF-01165.01-A, awarded by the Space Telescope Science Institute, which is operated by the Association of Universities for Research in Astronomy, Inc., for NASA, under contract NAS 5-26555. The DEIMOS spectrograph was funded by a grant from CARA (Keck Observatory), an NSF Facilities and Infrastructure grant (AST92-2540), the Center for Particle Astrophysics and by gifts from Sun Microsystems and the Quantum Corporation. The data presented herein were obtained at the W.M. Keck Observatory, which is operated as a scientific partnership among the California Institute of Technology, the University of California and the National Aeronautics and Space Administration. The Observatory was made possible by the generous financial support of the W.M. Keck Foundation. The DEEP2 team and Keck Observatory acknowledge the very significant cultural role and reverence that the summit of Mauna Kea has always had within the indigenous Hawaiian community and appreciate the opportunity to conduct observations from this mountain.

REFERENCES

Abazajian, K., et al. 2005, ApJ, 625, 613
Alimi, J.-M., Valls-Gabaud, D., & Blanchard, A. 1988, A&A, 206, L11
Allen, P. D., et al. 2005, MNRAS, 360, 1244
Benoist, C., et al. 1996, ApJ, 472, 452
Coil, A. L., et al. 2004a, ApJ, 609, 525
Coil, A. L., et al. 2006, ApJ, 638, in press
Coil, A. L., Newman, J. A., Kaiser, N., Davis, M., Ma, C., Kocevski, D. D., & Koo, D. C. 2004b, ApJ, 617, 765
Conroy, C., Wechsler, R. H., & Kravtsov, A. V. 2006, Submitted to ApJ (astro-ph/0512234)
Croton, D. J., et al. 2004, MNRAS, 352, 1232
Davis, M., et al. 2003, Proc. SPIE, 4834, 161 (astro-ph 0209419)
Davis, M., & Peebles, P. J. E. 1983, ApJ, 267, 465
Davis, M., Gerke, B. F., & Newman, J. A. 2004, In Proceedings of "Observing Dark Energy: NOAO Workshop", Mar 18-20, 2004
Faber, S., et al. 2003, Proc. SPIE, 4841, 1657
Faber, S., et al. 2006, in preparation
Hamilton, A. J. S. 1988, ApJ, 331, L59
Kravtsov, A. V., Berlind, A. A., Wechsler, R. H., Klypin, A. A., Gottlöber, S., Allgood, B., & Primack, J. R. 2004, ApJ, 609, 35
Landy, S. D., & Szalay, A. S. 1993, ApJ, 412, 64
Lee, K.-S., et al. 2005, Accepted to ApJ (astro-ph/0508090)
Marinoni, C., et al. 2005, A&A, 442, 801
Mo, H. J., & White, S. D. M. 1996, MNRAS, 282, 347
Norberg, P., et al. 2001, MNRAS, 328, 64
Norberg, P., et al. 2002, MNRAS, 332, 827
Ouchi, M., et al. 2005, Submitted to ApJL (astro-ph/0508083)
Peacock, J. A., et al. 2001, Nature, 410, 169
Peacock, J. A., & Dodds, S. J. 1994, MNRAS, 267, 1020
Peebles, P. J. E. 1980. The Large-Scale Structure of the Universe, Princeton, N.J., Princeton Univ. Press
Phleps, S., Peacock, J. A., Meisenheimer, K., & Wolf, C. 2005, submitted to A& A (astro-ph/0506320)
Pollo, A., et al. 2006, Submitted to A&A (astro-ph/0512429)
Roche, N., & Eales, S. A. 1999, MNRAS, 307, 703
Sheth, R. K., & Tormen, G. 1999, MNRAS, 308, 119
Smith, R. E., et al. 2003, MNRAS, 341, 1311
Tinker, J. L., Weinberg, D. H., Zheng, Z., & Zehavi, I. 2005, ApJ, 631, 41
Verde, L., et al. 2002, MNRAS, 335, 432
Willmer, C., et al. 2006, accepted to ApJ, astro-ph/0506041
Willmer, C. N. A., da Costa, L. N., & Pellegrini, P. S. 1998, AJ, 115, 869

Yan, R., Madgwick, D. S., & White, M. 2003, ApJ, 598, 848
Yan, R., White, M., & Coil, A. L. 2004, ApJ, 607, 739
Yang, X., Mo, H. J., Jing, Y. P., & van den Bosch, F. C. 2005, MNRAS, 358, 217
Zehavi, I., et al. 2004, ApJ, 608, 16
Zehavi, I., et al. 2005, ApJ, 630, 1